JOURNAL OF COMPUTATIONAL PHYSICS 103, 442–449 (1992)

A Constrained Moving Finite Element Solution of the One-Dimensional Oxygen Diffusion with Absorption Problem

R. O. MOODY

AEA Petroleum Services, Winfrith Technology Centre, Dorchester, Dorset DT2 8DH, United Kingdom

AND

M. J. BAINES

University of Reading, Department of Mathematics, P.O. Box 220, Reading RG6 2AX, United Kingdom

Received December 5, 1990; revised January 21, 1992

We derive an adaptive finite-element method for the numerical solution of a one-dimensional, implicit, moving-boundary problem: The *oxygen diffusion with absorption problem* of Crank and Gupta. The method, which includes a moving grid and incorporates an iteration for the velocity of the moving boundary, produces good results over a range of parameters. We present numerical and graphical results in one dimension and indicate an extension of the method to two dimensions.

1. INTRODUCTION

The *oxygen diffusion with absorption problem* [1, 2], a moving-boundary problem which has inspired much interest among numerical workers in recent years, is concerned with the absorption and diffusion of oxygen in tumour tissue. In the first stage of the problem, oxygen diffuses into and is absorbed by the tissue until a steady state is attained. The oxygen in-flow boundary is then sealed, causing the gas content to be reduced to zero by the continuing absorption process. A non-dimensionalised mathematical formulation of the second stage of the problem in terms of the concentration of oxygen, u, is

$$u_t = u_{xx} - 1, \qquad 0 < x < s(t), \quad 0 < t < T, \tag{1.1}$$

$$u_x = 0, \qquad x = 0, \quad 0 < t < T, \tag{1.2}$$

$$\left.\begin{aligned} u &= 0 \\ u_x &= 0 \end{aligned}\right\}, \qquad x = s(t), \quad 0 < t < T, \tag{1.3}$$

$$u = \tfrac{1}{2}(1-x)^2, \qquad 0 \leqslant x \leqslant s(0) \equiv 1, \quad t = 0. \tag{1.4}$$

The moving-boundary problem defined by (1.1)–(1.4) is closely related to Stefan problems (concerned with heating and melting), in which the dependent variable is temperature. The main difference between the current problem and Stefan problems is that the second equation of (1.3) is typically replaced by

$$u_x = -L\dot{s}(t), \qquad x = s(t), \quad 0 < t < T, \tag{1.5}$$

(where L is constant) in Stefan problems, thereby providing an explicit expression for $\dot{s}$, the velocity of the moving boundary. An adaptation of the present numerical method to solve one-phase Stefan problems is outlined in Section 3.

There are three factors which render (1.1)–(1.4) difficult to treat numerically: first, the initial data, (1.4), is inconsistent with the fixed-boundary condition, (1.2); second, there is no explicit expression for the velocity of the moving boundary; and third, this velocity becomes infinite in magnitude as the time, T, at which zero oxygen remains is approached. The first difficulty may be overcome by implementing a short-time analytic solution [1]; however, the present numerical method exhibits no instability when started at the initial time. The other difficulties, which occur at the moving boundary, require special treatments, and we describe these in Section 3.

Crank [3] reviews the numerous numerical methods that have been employed to solve the problem, (1.1)–(1.4), to which there is no known analytic solution. We merely mention the more important contributions, including the original finite-difference method of Crank and Gupta [1], which incorporates Lagrangian interpolation formulae and a node-deletion algorithm. In their subsequent method [2], they perform interpolations using cubic splines and cubic polynomials, and use a grid which moves with the velocity of the moving boundary. Gupta [4] avoids the use of the interpolation techniques of Crank and Gupta [1, 2] by

0021-9991/92 $5.00

implementing a Taylor expansion in both the space and time variables. Hansen and Hougaard [5] derive an integral-equation formulation for the position of the moving boundary and an integral formula for the concentration, solving using asymptotic and numerical techniques. The transformation of Landau [6],

$$\xi = x/s(t), \tag{1.6}$$

which maps the time-dependent domain $0 \leqslant x \leqslant s(t)$ onto the fixed region $0 \leqslant \xi \leqslant 1$, is included in the first method of Ferriss and Hill [7]; their second method involves the replacement of the moving-boundary conditions, (1.3), by the fixed-end condition

$$u_x = f(t), \qquad x = 1, \quad 0 < t < T, \tag{1.7}$$

where f is an unknown function which they determine. Berger *et al.* [8] solve the problem using the truncation method, a fixed-domain method in which negative solution values are *truncated* to zero. An important class of methods is that of variational inequalities, in which the original problem is reformulated as a fixed-domain problem and solved in an approximation space. These methods are considered by Baiocchi and Pozzi [9] and Elliott and Ockendon [10].

Miller *et al.* [11] solve the problem using an iterative finite-element method on an adaptive mesh, the number of nodes of which is automatically reduced in order to follow the inward motion of the moving boundary. A variable-time-step method is considered by Gupta and Kumar [12]: they select time increments which ensure that the moving boundary is located at a nodal point at each time level. Dahmardah and Mayers [13] express the concentration variable in terms of a Fourier series, which they truncate and then evaluate. The moving finite element method [14–16] is used by Moody [17] in his numerical solution of the problem.

In the present work, we employ a finite-element method on a moving grid to solve the oxygen diffusion with absorption problem, (1.1)–(1.4). The derivation of the method and its practical implementation are presented in Sections 2 and 3. Section 4 contains numerical and graphical results and discussion. In Section 5, we draw our conclusions and suggest how the method may be extended to solve a two-dimensional version of the problem.

2. NUMERICAL METHOD

The proposed front-tracking method presented in this paper is a constrained form of the moving finite element method of Miller and Miller [14] and Miller [15], which is further analysed by Wathen and Baines [18] and Baines and Wathen [19]. In this section, we describe the method (designated the constrained moving finite element method) and derive the corresponding discretised set of linear equations.

2.1. *Derivation of the Method*

We seek a piecewise-linear approximant, v, to the true solution, u, of the problem, (1.1)–(1.4), in the form

$$v = \sum_{j=1}^{N} a_j \alpha_j, \tag{2.1}$$

where $a_j = a_j(t)$, $j = 1, 2, ..., N$, are the numerical amplitudes corresponding to the time-dependent nodal positions $s_j = s_j(t)$, $j = 1, 2, ..., N$ (collectively represented by the vector $\mathbf{s}(t)$); and $\alpha_j = \alpha_j(x, \mathbf{s}(t))$, $j = 1, 2, ..., N$, are the standard piecewise-linear basis functions of local compact support. A typical interior α-type basis function is shown in Fig. 1.

Differentiation of (2.1) with respect to time results in the expression

$$v_t = \sum_{j=1}^{N} \{\dot{a}_j \alpha_j + \dot{s}_j \beta_j\}, \tag{2.2}$$

in which $\beta_j = \beta_j(x, \mathbf{s}(t), \mathbf{a}(t))$, $j = 1, 2, ..., N$, are (in general) discontinuous piecewise-linear basis functions. It is shown in [14, 20] that

$$\left.\begin{aligned} \beta_1 &= -m_{3/2}\alpha_1, \qquad x \in (s_1, s_2) \\ \beta_j &= \begin{cases} -m_{j-1/2}\alpha_j, & x \in (s_{j-1}, s_j) \\ -m_{j+1/2}\alpha_j, & x \in (s_j, s_{j+1}) \end{cases}, \\ & \quad j = 2, 3, ..., N-1 \\ \beta_N &= -m_{N-1/2}\alpha_N, \qquad x \in (s_{N-1}, s_N) \end{aligned}\right\}, \ t \geqslant 0, \tag{2.3}$$

where $m_{j-1/2}$ denotes the local slope of v in the element (s_{j-1}, s_j). A typical interior β-type basis function is shown in Fig. 2.

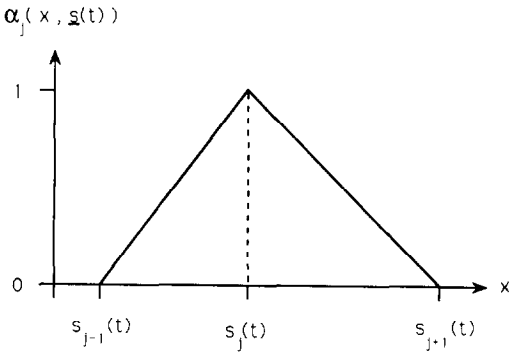

FIG. 1. The basic function α_j.

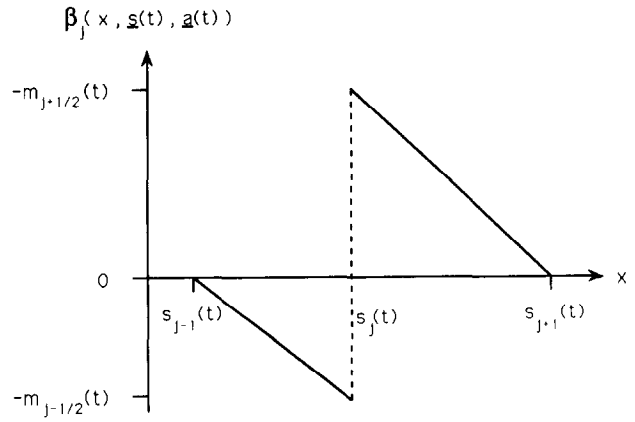

FIG. 2. The basis function β_j.

Let

$$N_{L_2} = \|v_t - v_{xx} + 1\|_2^2 \tag{2.4}$$

be the square of the global L_2-norm of the residual. Note that when v is piecewise linear, N_{L_2} of (2.4) is to be interpreted by considering v to be the limit of a sequence of smooth functions (see [14, 15]). When applying the finite element method to fixed-boundary problems with Neumann boundary conditions, it is standard procedure to implement the Galerkin equations, which may be considered as being obtained by minimising N_{L_2} over $\dot{a}_j$, $j = 1, 2, ..., N$. In our case, however, the right-hand boundary moves with a velocity which is determined only implicitly, although the value of the solution at this boundary is prescribed by the first of (1.3). We therefore minimise N_{L_2} not only over $\dot{a}_j$, $j = 1, 2, ..., N$, but also over $\dot{s}_N$, and obtain

$$\langle \alpha_i, v_t - v_{xx} + 1 \rangle = 0, \qquad i = 1, 2, ..., N, \tag{2.5a}$$

and

$$\langle \beta_N, v_t - v_{xx} + 1 \rangle = 0, \tag{2.5b}$$

where $\langle \cdot, \cdot \rangle$ is defined by

$$\langle f_1, f_2 \rangle = \int_{s_1}^{s_N} f_1(x) f_2(x)\, dx,$$

in which f_1 and f_2 are integrable functions.

Substitution of v_t from (2.2) into (2.5a), (2.5b) produces the semi-discrete system of equations

$$\sum_{j=1}^{N} \{\langle \alpha_i, \alpha_j \rangle \dot{a}_j + \langle \alpha_i, \beta_j \rangle \dot{s}_j - \langle \alpha_i, v_{xx} - 1 \rangle\} = 0, \qquad i = 1, 2, ..., N, \tag{2.6a}$$

and

$$\sum_{j=1}^{N} \{\langle \beta_N, \alpha_j \rangle \dot{a}_j + \langle \beta_N, \beta_j \rangle \dot{s}_j - \langle \beta_N, v_{xx} - 1 \rangle\} = 0. \tag{2.6b}$$

As β_j is discontinuous at s_j (see (2.3)), the integrals involving β_j are evaluated by splitting the interval $[s_{j-1}, s_{j+1}]$ into $[s_{j-1}, s_j]$ and $[s_j, s_{j+1}]$, then considering the restriction of β_j (defined in (2.3)) to each of these subintervals. The inner products involving the v_{xx} terms are evaluated using the usual integration-by-parts technique, in which the Neumann boundary conditions ((1.2) and the second of (1.3)) are imposed weakly.

The left-hand boundary is stationary and the right-hand one moves with a velocity which is determined through (2.6b). We eliminate the possibility of nodes colliding by constraining their velocities; namely, by specifying them in proportion to their nodal positions:

$$\dot{s}_j = (s_j / s_N)\, \dot{s}_N, \qquad j = 2, 3, ..., N-1. \tag{2.7}$$

Similar strategies for prescribing internal nodal velocities are considered by Lynch [20], Murray and Landis [21], and O'Neill and Lynch [22]. As the value of the moving-boundary velocity, $\dot{s}_N$, is not known a priori, we calculate its value using an iteration algorithm, details of which are presented in Section 3.

The nodes, s_j, $j = 1, 2, ..., N$, are initially equi-spaced on the interval $[0, 1]$; the corresponding initial amplitudes, a_j, $j = 1, 2, ..., N$, are obtained by minimising

$$\left\| u - \sum_{j=1}^{N} a_j \alpha_j \right\|_2^2, \qquad 0 \leqslant x \leqslant 1, \quad t = 0,$$

over these variables, then inverting the resulting tridiagonal system using a standard solver.

We now describe the formation of the discrete equations for the internal nodal amplitudes at each time level; in Section 3, we discuss the determination of the concentration at the moving boundary and the boundary velocity.

2.2. *Formation of the Discrete Equations*

The local-compact-support property of the α-type and β-type basis functions, together with (2.3), enables us to express (2.6a) (for an internal node s_i) in the *generic* form

$$\Delta_s \dot{a} - \Delta_a \dot{s} = \Delta_a / \Delta_s - \Delta_s, \tag{2.8}$$

since, for example,

$$\left.\begin{aligned} \langle \alpha_i, \alpha_i \rangle &= \tfrac{1}{3}[(s_i - s_{i-1}) + (s_{i+1} - s_i)] \\ \langle \alpha_i, \beta_i \rangle &= \tfrac{1}{3}[(a_i - a_{i-1}) + (a_{i+1} - a_i)] \end{aligned}\right\}, \qquad i = 2, 3, ..., N-1. \tag{2.9}$$

Here, a and s represent nodal values and positions respectively, and Δ_a and Δ_s denote differences. We now perform a splitting with weight θ $(0 \leqslant \theta \leqslant 1)$ to the Δ_a quantities in (2.8) to yield

$$\Delta_s^n \dot{a}^{n+\theta} - [\theta \Delta_a^{n+1} + (1-\theta)\Delta_a^n]\dot{s}^{n+\theta} = [\theta \Delta_a^{n+1} + (1-\theta)\Delta_a^n]/\Delta_s^n - \Delta_s^n, \quad (2.10)$$

where the n and $n+1$ superscripts denote evaluation at the present time level and the next one, respectively. Alternatively, we could apply the splitting technique to both Δ_a and Δ_s in (2.8); in practice, however, such an approach is slightly more complicated to implement and produces results which are virtually identical to those obtained using the present approach.

The amplitudes are advanced in time by replacing their velocities in (2.10) by the Euler formula; namely,

$$\dot{a}^{n+\theta} = [a^{n+1} - a^n]/\Delta t^{n+1/2}, \quad (2.11)$$

in which

$$\Delta t^{n+1/2} = t^{n+1} - t^n \quad (2.12)$$

is the time increment.

Substitution of (2.11) into the equation of which (2.10) is the generic form produces

$$T_{i-1}^n a_{i-1}^{n+1} + T_i^n a_i^{n+1} + T_{i+1}^n a_{i+1}^{n+1} = R_i^n, \qquad i = 2, 3, \ldots, N-1, \quad (2.13)$$

where T_{i-1}^n, T_i^n, T_{i+1}^n, and R_i^n are coefficients which are independent of the unknown amplitudes. (Explicit expressions for these coefficients for general nodal positions and velocities appear in Appendix 1.) An equation similar to one of (2.13) is obtained for the amplitude, a_1^{n+1}, at the fixed boundary. These $N-1$ equations, together with a special equation for the concentration at the moving boundary (discussed in detail in the following section), form a tridiagonal system.

In practice, we choose

$$\theta = \tfrac{1}{2}, \quad (2.14)$$

and so restrict our ensuing analysis to this particular case.

3. TREATMENT AT THE MOVING BOUNDARY

In this section we derive equations for the concentration at, and the velocity of, the moving boundary. We also describe the moving-boundary-velocity iteration procedure and the determination of time increments.

Miller *et al.* [11] deduce from the two conditions, (1.3), at the moving boundary that the solution is locally quadratic, of the form

$$u = \lambda[s(t) - x]^2, \qquad \lambda \in \mathbb{R}, \quad (3.1)$$

in a small neighbourhood of this boundary. Assuming this form to hold in the element closest to the moving boundary, they then exploit the local least-squares linear fit to (3.1),

$$g = -\lambda h_{N-1/2}[x - s(t) + h_{N-1/2}] + \tfrac{5}{6}\lambda h_{N-1/2}^2 \quad (3.2)$$

(where $h_{N-1/2}$ denotes the length of the rightmost element). This straight line, (3.2), crosses the zero-concentration line at

$$x = s(t) - \tfrac{1}{6}h_{N-1/2}.$$

They deduce that the relationship

$$a_N = -\tfrac{1}{5}a_{N-1} \quad (3.3)$$

holds in the last element, and this situation is depicted in Fig. 3. Following Miller *et al.* [11], we use (3.3) to model the homogeneous Dirichlet condition in (1.3). Note that this treatment is consistent with the projection of the initial function, as described in Section 2.1.

The θ-splitting technique, defined by Eq. (2.10), is also applied to (2.6b) to produce

$$A^n - B^n[\dot{s}_{N-1}^{n+1/2} + 2\dot{s}_N^{n+1/2}] - C^n = 0. \quad (3.4)$$

Here, A^n, B^n, and C^n are independent of nodal velocities but depend on unknown amplitudes. The velocity $\dot{s}_{N-1}^{n+1/2}$ may be

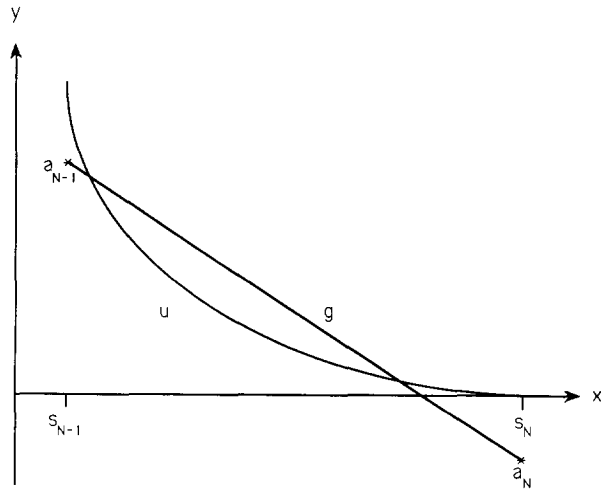

FIG. 3. The assumed quadratic form of the analytic solution, u, and its least-squares fit, g, in the last element.

expressed in terms of $\dot{s}_N^{n+1/2}$ using Eq. (2.7), enabling us to write

$$\dot{s}_N^{n+1/2} = (A^n + C^n)/D^n, \tag{3.5}$$

where D^n is a function of N and B^n. (Forms of A^n, B^n, C^n, and D^n with the general θ and arbitrary element lengths are stated in Appendix 2.) As A^n, B^n, and C^n are functions of the unknown amplitudes a_{N-1}^{n+1} and a_N^{n+1}, the following iteration algorithm is performed at each time level:

(i) Estimate $(\dot{s}_N^{n+1/2})_0$; set $l = 0$.

(ii) Determine $(\dot{s}_i^{n+1/2})_l$, $i = 2, 3, ..., N-1$.

(iii) Form a linear system for $(\mathbf{a}^{n+1})_l$.

(iv) Solve the system for $(\mathbf{a}^{n+1})_l$.

(v) Investigate the convergence of the iteration.

(vi) If necessary, obtain $(\dot{s}_N^{n+1/2})_{l+1}$ and return to (ii), with l replaced by $l+1$.

(vii) Update the nodal positions.

Owing to the negligible velocity of the moving boundary in its initial stages [5], we choose

$$(\dot{s}_N^{n+1/2})_0 = 0, \qquad n = 0, 1, \tag{3.6}$$

in (i). At subsequent time levels, we obtain an initial estimate of the moving-boundary velocity as follows. The amplitudes at the moving boundary and penultimate node are predicted from

$$\begin{aligned} a_j^{n+1} \simeq [&(\Delta t^{n-1/2} + \Delta t^{n+1/2})\, a_j^n \\ &- \Delta t^{n+1/2} a_j^{n-1}]/\Delta t^{n-1/2}, \\ &j = N-1, N, \end{aligned} \tag{3.7}$$

obtained by truncating Taylor expansions about time level n. The approximate amplitudes of (3.7) are then substituted into the expressions for A^n, B^n, C^n, and D^n, from which the boundary velocity is estimated using (3.5).

Stage (ii) of the algorithm is provided for via (2.7), and (iii) is achieved using the scheme defined by (2.13), together with a similar equation for a_1^{n+1} and (3.3). The new amplitudes in stage (iv) are obtained using a standard tridiagonal-matrix solver.

Having determined $(a_i^{n+1})_l$, $i = 1, 2, ..., N$, on the lth iteration at the nth time level, we form a corrected estimate of the moving-boundary velocity, $(\dot{s}_N^{n+1/2})_l^c$, using these amplitudes in (3.5). Convergence is then investigated numerically via

$$\begin{aligned} &|(\dot{s}_N^{n+1/2})_l - (\dot{s}_N^{n+1/2})_l^c| \\ &\quad < \varepsilon \max\{|(\dot{s}_N^{n+1/2})_l|, 1\}, \end{aligned} \tag{3.8}$$

(which allows for a zero, or almost zero, boundary velocity) in which ε is the iteration tolerance. If (3.8) is not satisfied then a further estimate for the velocity is provided for in stage (vi) by

$$(\dot{s}_N^{n+1/2})_{l+1} = \omega(\dot{s}_N^{n+1/2})_l^c + [1-\omega](\dot{s}_N^{n+1/2})_l, \tag{3.9}$$

where ω is a relaxation parameter. In practice, at most two iterations are required with the choices

$$\varepsilon = 5 \times 10^{-4}, \qquad \omega = \tfrac{1}{2}, \tag{3.10}$$

the second iteration being required only during the later stages of the absorption/diffusion process.

After obtaining a converged value for the moving-boundary velocity, we update the nodal positions in stage (vii), using the Euler formula (see (2.11)).

As t approaches T, the time at which zero oxygen remains, the velocity of the moving boundary becomes very large in magnitude. For this reason, we restrict the time increment to preserve accuracy of the numerical solution, using the following treatment. At each time level, the difference between the new and present positions of the moving boundary is not permitted to exceed a given multiple of the present one; i.e.,

$$|s_N^{n+1} - s_N^n| \leqslant \phi s_N^n, \tag{3.11}$$

for some ϕ. A first-order Taylor expansion of (3.11), using the previous boundary velocity as an approximation to the present one, yields

$$\Delta t^{n+1/2} \leqslant \phi s_N^n / |\dot{s}_N^{n-1/2}|. \tag{3.12}$$

We take the number of elements into consideration by choosing

$$\phi = \chi/(N-1), \tag{3.13}$$

where χ is a specified accuracy, given here by

$$\chi = 0.1 \tag{3.14}$$

for a 10% level. The time increment at each time level, n, is assigned using

$$\Delta t^{n+1/2} = \min\{\Delta t_{\max}, s_N^n/[10(N-1)\,|\dot{s}_N^{n-1/2}|]\}, \tag{3.15}$$

in which

$$\Delta t_{\max} = 10^{-4}. \tag{3.16}$$

We conclude Section 3 by describing a modification of the present method which would admit its application to a

one-phase Stefan problem. A major difference between the two problems lies in the condition at the moving boundary: the Stefan problem typically includes (1.5) in place of the second of (1.3). A discretisation of this condition gives rise to an equation for $\dot{s}_N$; Eq. (2.6b), obtained by minimising N_{L_2} over $\dot{s}_N$, is therefore redundant. It is generally easier to implement explicit conditions arising from (1.5) than it is to implement those arising from implicit conditions, such as the second of (1.3). The constrained moving finite element method may therefore be readily utilised to obtain numerical solutions to one-phase Stefan problems.

4. PRESENTATION AND ANALYSIS OF RESULTS

Numerical solutions of the oxygen diffusion with absorption problem, (1.1)–(1.4), are obtained using the parameters θ, ε, ω, χ, and $\Delta t_{\max}$ of Eqs. (2.14), (3.10), (3.14), and (3.16). Robustness of the method is illustrated by obtaining infrequent, negligible deviations in the numerical values when the iteration convergence tolerance, ε in (3.10), is decreased by two orders of magnitude.

In Fig. 4 we see numerical oxygen-concentration profiles at non-dimensional times of 0.00, 0.01, 0.05, 0.10, 0.15, and 0.19 when solving with 21 nodes. The solid diamonds, joined by the linear segments, denote the nodal concentrations, which decrease with time. The minute initial and large final velocities of the boundary are apparent in Fig. 5, in which the variation of the position of the boundary with time is displayed.

The nature of the problem is such that zero oxygen remains in the tumour tissue after a time T. Values of 0.197050, 0.197424, and 0.197417 for T are obtained from 11-, 21-, and 41-node solutions, respectively, suggesting a final time of approximately 0.19742 non-dimensional units. (In these three cases, the magnitudes of the moving-boundary position, moving-boundary velocity, and fixed-boundary concentration at the final time are $O(10^{-18})$, $O(10^{18})$, and $O(10^{-37})$, respectively.) Our value for the final time compares favourably with those of previous workers: 0.1972–0.1977, of Hansen and Hougaard [5]; 0.196–0.198, of Miller *et al.* [11]; 0.19732 and 0.19734, of Gupta and Kumar [12]; and 0.197434, of Dahmardah and Mayers [13].

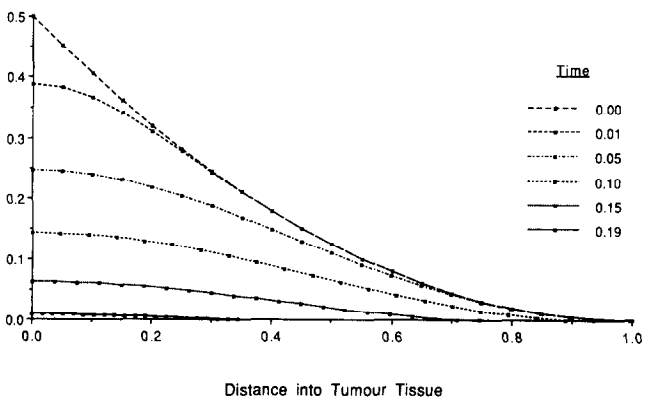

FIG. 4. Numerical oxygen-concentration profiles at selected times.

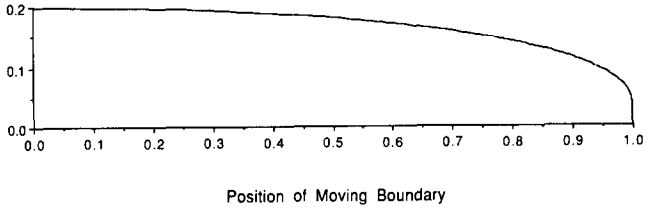

FIG. 5. Variation of moving-boundary position with time.

Tables I and II respectively contain the numerical values of Dahmardah and Mayers [13] (which are generally considered to be the most accurate available) for the moving-boundary position and fixed-boundary oxygen concentration at selected times. Also included in the tables are the deviations from the values in [13] of those of the constrained moving finite element method when solving with 11, 21, and 41 nodes.

With reference to Table I, we see that there is no deviation in the two sets of results up to and including a time of 0.02. After this time, the results of the constrained moving finite element method exceed the comparison values slightly, then pass through a minimum deviation between 0.16 and 0.18. The present method then produces values which are less than those of Dahmardah and Mayers [13] until the final times. Generally, the deviations in moving-

TABLE I

Deviations in Computed Moving-Boundary Positions at Selected Times, as Compared with Those of Dahmardah and Mayers [13]

Time	Position in [13]	Deviation in position ($\times 10^5$)		
		11 Nodes	21 Nodes	41 Nodes
0.0100	1.00000	0	0	0
0.0200	1.00000	0	0	0
0.0300	0.99991	−11	−4	−1
0.0400	0.99918	−64	−18	−5
0.0500	0.99679	−144	−38	−10
0.1000	0.93502	−420	−106	−24
0.1200	0.87917	−420	−105	−22
0.1400	0.79894	−349	−85	−15
0.1600	0.68345	−181	−39	0
0.1800	0.50133	194	61	31
0.1900	0.34600	700	124	47
0.1950	0.20845	1579	133	91
0.1960	0.16313	2257	135	127
0.1970	0.09305	6020	154	196
0.1972	0.06944	—	181	271
0.1974	0.02782	—	459	831

boundary position decrease on increase in the number of nodes for a fixed time; this is not the case, however, for the 21-node and 41-node results after a time of 0.196.

The deviations in concentration at the fixed boundary in Table II are, in general, much lower than their moving-boundary-position counterparts. These results behave in a similar manner to those in Table I, exhibiting a minimum deviation between 0.05 and 0.10. Note that the 21-node and 41-node results are in excellent agreement with each other throughout, but especially so at later times (when the problem is at its most severe).

When compared with the results in [13], our results are generally at least as accurate as those from any other method mentioned in this paper. The deviations in Tables I and II illustrate that the numerical results of the constrained moving finite element method are approximately second-order accurate with respect to the comparison values until a time of 0.19; after this time, the order is unreliable. The reduction in accuracy may be due to the fact that the (unknown) analytic solution can no longer be adequately approximated by a quadratic over the whole extent of the last element after a time of 0.19; in this case, a higher-order polynomial-fit may be more appropriate. With an assumed form of

$$g = \lambda[s(t) - x]^p, \qquad \lambda \in \mathbb{R}, \quad p \in \mathbb{N}, \tag{4.1}$$

the condition corresponding to (3.3) is

$$a_N = -\frac{(p-1)}{(2p+1)} a_{N-1}. \tag{4.2}$$

TABLE II

Deviations in Computed Fixed-Boundary Concentrations at Selected Times, as Compared with Those of Dahmardah and Mayers [13]

Time	Concentration in [13]	Deviation in concentration ($\times 10^5$) 11 Nodes	21 Nodes	41 Nodes
0.0100	0.38716	−160	−39	−10
0.0200	0.34042	−86	−21	−5
0.0300	0.30456	−54	−13	−3
0.0400	0.27432	−36	−9	−3
0.0500	0.24769	−22	−5	−1
0.1000	0.14318	15	4	1
0.1200	0.10913	23	5	1
0.1400	0.07785	31	7	1
0.1600	0.04882	37	8	1
0.1800	0.02178	43	9	1
0.1900	0.00902	45	6	1
0.1950	0.00288	44	2	1
0.1960	0.00169	46	2	3
0.1970	0.00049	43	0	1
0.1972	0.00027	—	1	2
0.1974	0.00004	—	1	2

With a sufficiently large value of p, the inclusion of (4.2) in place of (3.3) may restore the second-order accuracy of the method after a time of 0.19. It may be advantageous to smoothly vary the boundary equation from (3.3) to

$$a_N = -\tfrac{1}{2} a_{N-1} \tag{4.3}$$

(which is the limiting form of (4.2) as p tends to infinity) as time increases from 0.19 to T. Of course, this approach would not be successful if (4.1) were distant from the correct form of the analytic solution in the vicinity of the moving boundary; for example, a more complicated polynomial, an exponential, or even an error function might be more appropriate.

The c.p.u. times consumed on a Norsk-Data Nord 500 mini computer when using 11, 21, and 41 nodes are approximately 8, 15, and 43 s, respectively. Although it is not generally possible to compare the speed of the constrained moving finite element method with speeds of rival methods (as different computers were used), the authors are in a position to ascertain that the current method is far quicker than that of Miller *et al.* [11].

5. CONCLUSIONS

We have described a constrained form of the moving finite element method and applied it to the one-dimensional oxygen diffusion with absorption problem. The numerical results indicate that the method is second-order accurate almost everywhere, and the low c.p.u. times reveal an inexpensive solution technique.

Current investigation consists of extending the numerical method to admit its application to a two-dimensional version of the problem, in which the second of (1.3) is valid in the normal direction at all points on the moving boundary. The algorithm of Section 3 will now include the solution of a linear system system of boundary velocities, obtained by applying (3.3) in the normal direction at each moving-boundary node. In this case, the value of a_{N-1} will have to be determined using interpolation techniques.

A future task will be to further modify the method so that it can be used to solve one- and two-dimensional Stefan problems. This work will be based on the discussion in Section 3.

APPENDIX 1

The generalised coefficients of Eq. (2.13) are

$$T^n_{i-1} = h^n_{i-1/2} + \theta\, \Delta t^{n+1/2}[2\dot{s}^{n+\theta}_i + \dot{s}^{n+\theta}_{i-1}] - 6\theta\, \Delta t^{n+1/2}/h^n_{i-1/2}, \tag{A.1}$$

$$T_i^n = 2[h_{i-1/2}^n + h_{i+1/2}^n] + \theta\,\Delta t^{n+1/2}[\dot{s}_{i+1}^{n+\theta} - \dot{s}_{i-1}^{n+\theta}] + 6\theta\,\Delta t^{n+1/2}[1/h_{i-1/2}^n + 1/h_{i+1/2}^n], \quad (A.2)$$

$$T_{i+1}^n = h_{i+1/2}^n - \theta\,\Delta t^{n+1/2}[2\dot{s}_i^{n+\theta} + \dot{s}_{i+1}^{n+\theta}] - 6\theta\,\Delta t^{n+1/2}/h_{i+1/2}^n, \quad (A.3)$$

$$\begin{aligned} R_i^n = {} & a_{i-1}^n\{h_{i-1/2}^n - (1-\theta)\,\Delta t^{n+1/2} \times [2\dot{s}_i^{n+\theta} + \dot{s}_{i-1}^{n+\theta}] + 6(1-\theta)\,\Delta t^{n+1/2}/h_{i-1/2}^n\} \\ & + a_i^n\{2[h_{i-1/2}^n + h_{i+1/2}^n] - (1-\theta)\,\Delta t^{n+1/2}[\dot{s}_{i+1}^{n+\theta} - \dot{s}_{i-1}^{n+\theta}] \\ & - 6(1-\theta)\,\Delta t^{n+1/2}[1/h_{i-1/2}^n + 1/h_{i+1/2}^n]\} \\ & + a_{i+1}^n\{h_{i+1/2}^n + (1-\theta)\,\Delta t^{n+1/2} \times [2\dot{s}_i^{n+\theta} + \dot{s}_{i+1}^{n+\theta}] + 6(1-\theta)\,\Delta t^{n+1/2}/h_{i+1/2}^n\} \\ & - 3\Delta t^{n+1/2}(h_{i-1/2}^n + h_{i+1/2}^n), \end{aligned} \quad (A.4)$$

in which

$$h_{i-1/2}^n = s_i^n - s_{i-1}^n. \quad (A.5)$$

APPENDIX 2

The generalised coefficients of Eqs. (3.4) and (3.5) are

$$A^n = h_{n-1/2}^n\{a_{N-1}^{n+1} - a_{N-1}^n + 2[a_N^{n+1} - a_N^n] + 3\Delta t^{n+1/2}\}, \quad (A.6)$$

$$B^n = \Delta t^{n+1/2}\{\theta[a_N^{n+1} - a_{N-1}^{n+1}] + (1-\theta)[a_N^n - a_{N-1}^n]\}, \quad (A.7)$$

$$C^n = 6\Delta t^{n+1/2}\{\theta[a_N^{n+1} - a_{N-1}^{n+1}] + (1-\theta)[a_N^n - a_{N-1}^n]\}/h_{N-1/2}^n, \quad (A.8)$$

$$D^n = B^n[3 - 1/(N-1)], \quad (A.9)$$

where $h_{N-1/2}^n$ is defined in (A.5).

ACKNOWLEDGMENTS

The authors thank Dr. C. P. Please, of the University of Southampton, for useful advice in connection with this work. The work described in this paper was carried out while the first author was in receipt of a Science and Engineering Research Council CASE Studentship in association with GEC.

REFERENCES

1. J. Crank and R. S. Gupta, *J. Inst. Math. Appl.* **10**, 19 (1972).
2. J. Crank and R. S. Gupta, *J. Inst. Math. Appl.* **10**, 296 (1972).
3. J. Crank, *Free and Moving Boundary Problems* (Clarendon Press, Oxford, 1984).
4. R. S. Gupta, *Comput. Methods Appl. Mech. Eng.* **4**, 143 (1974).
5. E. B. Hansen and P. Hougaard, *J. Inst. Math. Appl.* **13**, 385 (1974).
6. H. G. Landau, *Q. Appl. Math.* **8**, 81 (1950).
7. D. H. Ferriss and S. Hill, NAC45, National Physical Laboratory, Teddington, UK, 1974 (unpublished).
8. A. E. Berger, M. Ciment, and J. C. W. Rogers, *SIAM J. Numer. Anal.* **12**, 646 (1975).
9. C. Baiocchi and G. A. Pozzi, *Appl. Math. Opt.* **2**, 304 (1976).
10. C. M. Elliott and J. R. Ockendon, *Weak and Variational Methods for Moving Boundary Problems* (Pitman, London, 1982).
11. J. V. Miller, K. W. Morton, and M. J. Baines, *J. Inst. Math. Appl.* **22**, 467 (1978).
12. R. S. Gupta and D. Kumar, *Int. J. Heat Mass Transfer* **24**, 251 (1981).
13. H. O. Dahmardah and D. F. Mayers, *IMA J. Numer. Anal.* **3**, 81 (1983).
14. K. Miller and R. N. Miller, *SIAM J. Numer. Anal.* **18**, 1019 (1981).
15. K. Miller, *SIAM J. Numer. Anal.* **18**, 1033 (1981).
16. M. J. Baines, in *Numerical Methods for Fluid Dynamics II*, edited by K. W. Morton and M. J. Baines (Clarendon Press, Oxford, 1986).
17. R. O. Moody, 17/85, Department of Mathematics, University of Reading, 1985 (unpublished).
18. A. J. Wathen and M. J. Baines, *IMA J. Numer. Anal.* **5**, 161 (1985).
19. M. J. Baines and A. J. Wathen, *J. Comput. Phys.* **79**, 245 (1988).
20. D. R. Lynch, *J. Comput. Phys.* **47**, 387 (1982).
21. W. D. Murray and F. Landis, *J. Heat Transfer, Trans. Am. Soc. Mech. Eng. C* **81**, 106 (1959).
22. K. O'Neill and D. R. Lynch, in *Numerical Methods in Heat Transfer*, edited by R. W. Lewis, K. Morgan, and O. C. Zienkiewicz (Wiley, New York, 1981).